◆ Human Brain Mapping 37:678–688 (2016) ◆

Hindbrain Regional Growth in Preterm Newborns and its Impairment in Relation to Brain Injury

**Hosung Kim,[1] Dawn Gano,[2] Mai-Lan Ho,[3] Xiaoyue M. Guo,[4] Alisa Unzueta,[4] Christopher Hess,[1] Donna M. Ferriero,[2,4] Duan Xu,[1] and A. James Barkovich[1,4]*

[1]*Department of Radiology and Biomedical Imaging, University of California, San Francisco, California*
[2]*Department of Pediatrics, University of California, San Francisco, California*
[3]*Department of Radiollogy, Mayo Clinic, Rochester, MN*
[4]*Department of Neurology, University of California, San Francisco, California*

Abstract: Premature birth globally affects about 11.1% of all newborns and is a risk factor for neurodevelopmental disability in surviving infants. Histology has suggested that hindbrain subdivisions grow differentially, especially in the third trimester. Prematurity-related brain injuries occurring in this period may selectively affect more rapidly developing areas of hindbrain, thus accompanying region-specific impairments in growth and ultimately neurodevelopmental deficits. The current study aimed to quantify regional growth of the cerebellum and the brainstem in preterm neonates (n = 65 with individually multiple scans). We probed associations of the regional volumes with severity of brain injury. In neonates with no imaging evidence of injury, our analysis using a mixed-effect linear model showed faster growth in the pons and the lateral convexity of anterior/posterior cerebellar lobes. Different patterns of growth impairment were found in relation to early cerebral intraventricular hemorrhage and cerebellar hemorrhage ($P < 0.05$), likely explaining different mechanisms through which neurogenesis is disrupted. The pattern of cerebellar growth identified in our study agreed excellently with details of cerebellar morphogenesis in perinatal development, which has only been observed in histological data. Our proposed analytic framework may provide predictive imaging biomarkers for neurodevelopmental outcome, enabling early identification and treatment of high-risk patients. *Hum Brain Mapp 37:678–688, 2016.*

Key words: hindbrain regional growth; surface-based morphometry; neonatal brain MRI; preterm newborns

Contract grant sponsor: NIH; Contract grant numbers: R01EB009756, R01HD072074, P01NS082330, R01NS046432; Contract grant sponsors: Fonds de Recherche Santé Québec (FRSQ) and Banting Postdoctoral Fellowships (to H.K.).

*Correspondence to: A. James Barkovich, 1975 4th Street, C-1758L, San Francisco, CA 94158. E-mail: james.barkovich@ucsf.edu

Received for publication 1 July 2015; Revised 28 October 2015; Accepted 6 November 2015.

DOI: 10.1002/hbm.23058

Published online 21 November 2015 in Wiley Online Library (wileyonlinelibrary.com).

INTRODUCTION

Premature birth is an established risk factor for motor, cognitive, and behavioral disability in surviving infants; it affected approximately 520,000 newborns (11.1%) in 2010 [Blencowe et al., 2012]. Magnetic resonance imaging (MRI) is increasingly used to provide in vivo high-resolution images of the brain parenchyma in preterm newborns. Imaging evidence of supratentorial intraventricular hemorrhage, white matter injury, hydrocephalus and cerebellar hemorrhage is often found in preterm newborns, and has been associated with neuromotor and cognitive deficits in early childhood [Hoekstra et al., 2004; Miller et al., 2005]. However, association of low-grade injuries with neurodevelopmental outcome has not been evident [Imamura et al., 2013; Payne et al., 2013]. Delayed cerebellar growth in preterm newborns has been associated with imaging evidence of supratentorial and infratentorial hemorrhage. Cerebellar volumes have also been used as a predictor of short- and long-term developmental outcomes in preterm born children [Barkovich et al., 2001; Lind et al., 2011; Parker et al., 2008; Skiold et al., 2014; Van Kooij et al., 2012].

The cerebellum grows dramatically from 4 weeks post-conception through the early postnatal period. In particular, its growth rate is quite rapid when compared with the cerebrum during the last half of gestation and the first postnatal year [Knickmeyer et al., 2008; Rakic and Sidman, 1970; Sidman and Rakic, 1973]. Cerebellar cells initially develop from two germinal zones: the ventricular zone of the fourth ventricle, where the GABAergic Purkinje cells develop, and the rhombic lip that develops in the lateral walls of the roof of the fourth ventricle and produces glutamatergic granule cells [Gilthorpe et al., 2002; ten Donkelaar et al., 2003; Wang and Zoghbi, 2001]. In early embryo stages, granule cells migrate over the cerebellar surface to form the external granular layer (EGL), which is stimulated to generate new cells during late embryogenesis and early perinatal/postnatal period by sonic hedgehog secreted by Purkinje cell neurites that extend into the EGL. Thus, the EGL also functions as a germinal zone for granule cells and other glutamatergic neurons [Sotelo, 2004]. The granule cells in the EGL begin migration to their deeper definitive site, the internal granular layer, in late fetal development and early postnatal development until the second postnatal year [ten Donkelaar et al., 2003]. Animal studies have suggested that cerebellar subdivisions of EGL grow differentially due to distribution of Purkinje cells that spread primarily in the anteroposterior plane and cluster distinctively through differential molecular signaling [Dastjerdi et al., 2012]. A fetal histological study has also confirmed the different growth trajectories of cerebellar lobes, especially during the third trimester [Nowakowska-Kotas et al., 2014]. Brain injuries that occur in this period may have a greater effect upon cerebellar areas that grow more rapidly, resulting in region-specific impairments in cerebellar growth.

Animal and pathologic studies have revealed complex polysynaptic connections between the various cerebral cortical regions, deep gray cerebral nuclei, brainstem and cerebellum through cortico-ponto-cerebellar projections. Dysfunction in the cerebrum, brainstem or cerebellum, anywhere along these pathways, may thus disrupt such pathways [Geva et al., 2014; Van Braeckel and Taylor, 2013]. However, brainstem development has been rarely studied [Holland et al., 2014] and differences in premature infants are not well understood.

In vivo MRI with advanced image processing and morphometry is capable of assessing regional brain growth. Particularly, surface-based morphometry approaches demonstrate sensitivity to macroscopic changes of structural boundaries [Joo et al., 2014; Kim et al., 2013].

The goal of this study was to quantify the regional growth of the hindbrain in preterm neonates, and subsequently determine associations of growth perturbations with conventional imaging patterns of injury. As perinatal and postnatal clinical factors may affect cerebellar growth [Tam et al., 2011a], we also assessed their effects and included those with significant effects as covariates in our model in order to identify independent effects of imaging evidence of brain injury.

METHODS

Subjects

We studied 65 preterm newborns (mean postmenstrual age [PMA]= 28.6 ± 2.0 weeks; range 24.1-32.2 weeks) admitted to the neonatal intensive care nursery at the University of California, San Francisco (UCSF) between July 2011 and March 2015. Exclusion criteria included (i) clinical evidence of a congenital malformation or syndrome, (ii) congenital infection, and (iii) newborns too clinically unstable for transport to the MRI scanner. Parental consent was obtained for all cases following a protocol approved by the institutional Committee on Human Research. Customized MRI-compatible incubators with specialized head coils were used to provide a quiet, well-monitored environment for neonates, minimizing patient movement and improving the signal-to-noise ratio. All patients were scanned postnatally as soon as clinically stable, and 38 patients were rescanned before discharge at late preterm age (34-39 weeks corrected gestational age). Due to severe motion artifact, 9 baseline scans and 6 follow-up scans were excluded, leaving 56 baseline (PMA=32.4 ± 1.9 weeks) and 32 follow-up (36.1 ± 1.6 weeks) scans. No subject was however excluded among the initial 65 newborns who had an acceptable baseline or follow-up scan or both. Sedation was used only with parental consent and when subjects moved, resulting in imaging artifact. Approximately 50% of the cohort received sedation, usually pentobarbital in small doses.

MRI Acquisition

MRI scans were acquired on a 3-Tesla General Electric Discovery MR750 system (GE Medical Systems, Waukesha, WI, USA) using a specialized high-sensitivity neonatal head coil built within a custom-built MRI-compatible incubator. T1-weighted images were acquired using sagittal 3-dimensional inversion recovery spoiled gradient echo (3D IR-SPGR) (repetition time [TR]=minimum; echo time [TE]=minimum; inversion time of 450 ms; field of view [FOV]=180 mm; number of excitations [NEX]=1.00; Flip angle [FA]=15°), and were reformatted in the axial and coronal planes, yielding images with 0.7x0.7x1mm^3 spatial resolution, to look at surface anatomy and brain distortions due to malformation or prior (subacute to chronic) injury. Axial FSE-XL T2-weighted images were acquired to look for areas of encephalomalacia or malformations using the parameters TR=5000 ms; TE=120 ms; FOV=200 mm; NEX=2.0; slice thickness=3mm. Susceptibility-weighted images (SWI) were acquired to look for hemorrhages and calcifications with the parameters TR=46 ms; TE=28 ms; FA= 20°; FOV=180 mm; NEX=1.0; slice thickness=2.0 mm. The scan times for T1w, T2w and SWI were approximately 3.5, 2.5 and 5 minutes, respectively.

Diagnosis of Neonatal Brain Injuries

Two pediatric neuroradiologists (A.J.B., M-L.H) blinded to patient history reviewed patient MRI scans including 3-D T1 and axial T2-weighted sequences, as well as SWI when available (n = 30). Presence and severity of intraventricular hemorrhage (IVH), hydrocephalus (= ventriculomegaly), white matter injury (WMI), and cerebellar hemorrhage (CbH) was evaluated. Consensus scores were generated for IVH using the scoring system of Papile (0: absent; 1: germinal matrix hemorrhage; 2: intraventricular hemorrhage; 3: intraventricular hemorrhage with hydrocephalus; 4: parenchymal hemorrhage, usually periventricular hemorrhagic infarction) (Papile et al, 1978) and WMI (0: absent; 1: $<$3 foci, $<$2 mm; 2: $\geq$3 foci, $>$2 mm; 3: $>$5% hemisphere) using established criteria (Miller et al., 2003; Papile et al., 1978). The grading system for CbH was defined as: 0 (absent hemorrhage), 1 ($<$3 foci/$\leq$2 mm), 2 ($\geq$3 foci/3–5 mm), or 3 ($\geq$6 mm/$<$5% hemisphere). Subsequently, IVH scores were binarized with "mild" representing grades 1-2, and "severe" representing grades 3-4; WMI was categorized as "mild" for grade 1 and "severe" for grades 2-3. For subjects with multiple MR examinations, the highest (most severe) score in each category was used for analysis.

Image Preprocessing

Each image underwent automated correction for intensity non-uniformity [Sled et al., 1998] and was then spatially normalized using linear registration to a NIH-pediatric template for neonates at 0 to 2 months [Almli et al., 2007] using an unbiased framework for the construction of nonlinear average templates [Fonov et al., 2011].

Segmentation of the Hindbrain

Using the three-dimensional T1-weighted image data registered to standard stereotaxic space, boundaries of the hindbrain (pons, medulla and cerebellum) were manually delineated (Fig. 1). On sagittal images, a straight line connecting the caudalmost aspect of the inferior colliculus and rostralmost superior pons was used to define the superior border of the hindbrain. A horizontal line at the level of the top of the obex was used to define the inferior border of the hindbrain. We measured the inter-rater agreement between two imaging physicists using kappa-statistics (inter-rater agreement: $\kappa = 91 \pm 3\%$ for randomly chosen 15 cases). For the optimal segmentation, the two raters created a consensus of labeling each individual hindbrain for all cases.

Surface-Based Mapping of Hindbrain Growth

Using a nearest-neighborhood interpolation, hindbrain labels were mapped back to their native imaging space. A previously validated surface-based approach [Kim et al., 2008] was used to measure local volume changes by computing Jacobian determinants on surface-based displacement vectors between a given subject and a template surface [Styner et al., 2006]. Hindbrain segmentations were converted to surface meshes using a spherical parameterization (SPHARM) based on area-preserving, distortion-minimizing mapping. Using a uniform icosahedron-subdivision of the SPHARM, we obtained a point distribution model (PDM) to allow shape-inherent point correspondences across subjects (1,962 vertices). Each individual SPHARM-PDM surface was rigidly aligned to a template constructed from the mean surface of all subjects with respect to the centroid and longitudinal axes of the first-order ellipsoid [Gerig et al., 2001]. Vertex-wise displacement vectors were calculated between each individual and the overall template [Styner et al., 2006]. Displacement vectors were diffused within the volume enclosed by the surface using a heat equation, yielding a displacement vector field. To assess local volume changes, we calculated Jacobian determinants from these vector fields [Kim et al., 2008]. Jacobian determinants were projected back onto the template surface using tri-linear interpolation and, subtracting 1, we obtained a metric of growth ($J > 0$) or shrinkage ($J < 0$) in a unit-size cube defined on each vertex.

Statistical Analysis

Analysis was performed using SurfStat (http://www.math.mcgill.ca/keith/surfstat/) [Chung et al., 2010]. Mixed-effect linear models were used to address both inter-subject effects and within-subject changes between serial MR examinations by permitting multiple measurements per subject thereby increasing statistical power. We assessed hindbrain growth in patients with no imaging evidence of brain injury (n = 30) by correlating point-wise Jacobian

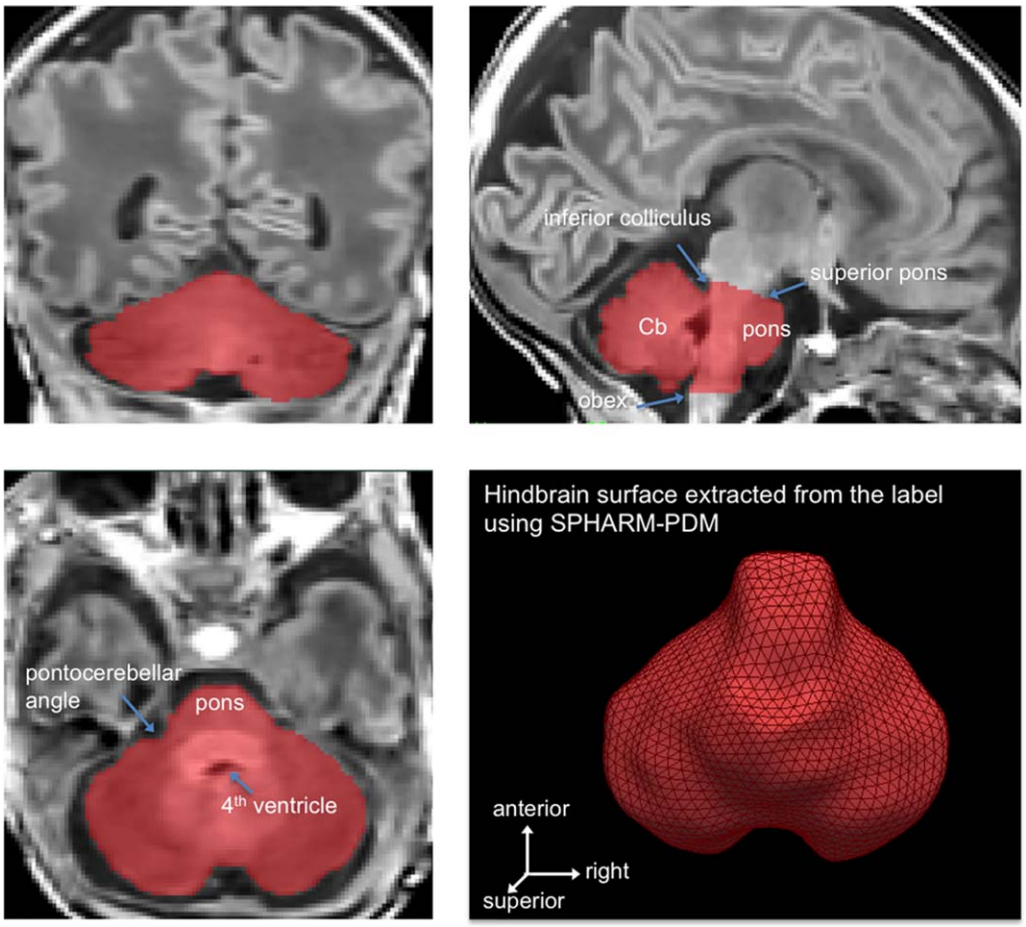

Figure 1.
Segmentation and surface extraction of the hindbrain, including the cerebellum, medulla, and pons. [Color figure can be viewed in the online issue, which is available at wileyonlinelibrary.com.]

metrics with postmenstrual age (PMA) at the time of scanning.

To assess associations between hindbrain growth and cerebral injury (IVH/WMI/hydrocephalus: binarized as none/mild *vs*. moderate/severe) or CbH (binarized as 0-1 vs. 2-3), at each surface point we analyzed an interaction term of IVH, WMI, CbH or hydrocephalus with the dependent variable set as volumes. For each form of injury, other types of injury were included as covariates in the model to account for possible confounding effects. Finally, the analysis of interaction term between an injury variable and PMA will assess the association of the given injury type to hindbrain growth.

For the analyses mentioned above, we also included covariates of the clinical variables that resulted in a significant correlation or association with hindbrain growth (when using univariate tests). This model was designed to control for the possible confounding effects of clinical variables in correlation.

Correction for Multiple Comparisons

In all surface analyses, significances were thresholded using the false discovery rate procedure [Benjamini and Hochberg, 1995], with FDR < 0.05.

Surface Mapping of Hindbrain Parcellation

Manual tracing of hindbrain subdivisions [Sato et al., 2015] was performed on two individual MRI examinations scanned at relatively late PMAs (39.7, 40.2 weeks), when regional anatomic boundaries were best delineated. The traced boundaries were interpolated on each subject's surface and subsequently transposed onto the surface template using the SPHARM-PDM point correspondence. The two tracings were averaged to approximate the final borders. To note, the entire hindbrain segmentation described in the previous section was used for subsequent surface extraction and regional volume measurement. The subdivisional labeling was, on the

TABLE I. Imaging data

Demographic	
Subjects (*n*)	65
MRI scans (*n*)	88
Sex: male (*n*)	32
GA at birth (wk, mean ± SD)	28.5 ± 2.0
PMA at MRI	
First scans	32.4 ± 1.8
Second scans	36.1 ± 1.6
Babies with imaging evidence of brain injuries (*n*)	35
IVH (mild/severe) (*n*)	10/7 (59/41%)
WHI (mild/severe) (*n*)	10/7 (59/41%)
Cerebellar hemorrhage (*n*)	25
Grade (1/2/3) (*n*)	14/7/4 (56/28/16%)
Laterality: unilateral/bilateral (*n*)	9/16 (36/64%)
Number of CbH (1–2 foci/3–5 foci/≥ 6 foci)	7/8/10 (28/32/40%)
Size of primary CbH (≤2 mm/3–5 mm/≥6 mm)	14/6/5 (56/24/20%)

other hand, used to project it onto the template surface and interpret findings according to the traced subregions.

RESULTS

Demographics and Clinical Parameters

Detailed demographics and clinical characteristics of the subjects were described in Tables I and II. The occurrence of moderate/severe CbH was not associated with that of moderate/severe IVH (Fisher's exact test; $P > 0.1$), with that of moderate/severe WMI ($P > 0.2$) or that of hydrocephalus ($P > 0.2$). Univariate analyses showed that the following clinical factors were associated with overall hindbrain growth ($P < 0.05$ adjusted using Bonferroni): birth weight, duration of mechanical ventilation, infection, and exposure to postnatal steroids. We therefore included these clinical variables as covariates in the following statistical tests.

Pattern of Hindbrain Growth in Preterm Neonates With no Brain Injury

Preterm neonates without imaging evidence of cerebral or cerebellar injuries demonstrated overall cerebellum and brainstem growth rates correlating with PMA (mean 0.7 mm^3/voxel per week; $t = 12.7$; $P < 0.0001$). Normal growth was faster in the pons and the anterior/posterior cerebellar lobes (0.8–0.9mm^3/voxel/week), and slower in the tonsils and vermis (0.3–0.6 mm^3/voxel/week; Fig. 2).

Association of Severe Brain Injury With Hindbrain Growth

Moderate/severe IVH and CbH were associated with slower cerebellar growth relative to no/mild injury types. Growth impairment due to brain injury was noted to affect the entire hindbrain relative to the growth without injury (IVH: -0.2 mm^3/voxel/week, $t = 2.5$, $P = 0.01$; CbH: $-0.3mm^3$/voxel/week, $t = 3.4$, $P < 0.001$). In cases of moderate/severe IVH, growth restriction mapped mainly to the dorsal superior lobe and pons (Fig. 3A). In patients with moderate/severe CbH, growth restriction was extensive across regions ($t > 2.8$; $P < 0.05$) and affected primarily the posterior inferior lobe, posterior vermis, and tonsil ($t > 5.5$; $P < 0.0001$; 0.1 mm^3/voxel/week; Fig. 3B). These were the regions involved by parenchymal hemorrhage, the distribution of which was more pronounced in superficial layers (0–3.5 mm in depth; Fig. 4). There was no significant association between cerebellar growth, and WMI or hydrocephalus ($P > 0.1$).

DISCUSSION

Our study investigated regional growth of the hindbrain in preterm born neonates and its impairment in relation to perinatal brain injuries. In neonates with no imaging evidence of supra- and infra-tentorial injuries, our analysis using a mixed-effect linear model showed faster growth in the pons and the lateral convexity of anterior/posterior cerebellar lobes. The postnatal hindbrain growth was

TABLE II. Clinical characteristics

Characteristic[a]	Number (%)
Maternal/antenatal factors	
Maternal age (yrs)	29.6 ± 7.0
Placenta previa	8 (12.3)
Maternal smoking[b]	3 (4.6)
Magnesium sulfate	44 (67.8)
Exposure to prenatal steroids	47 (72.3)
Placental abruption	9 (13.8)
Chorioamnionitis	14 (21.5)
Delivery/perinatal factors	
Twin	29 (44.0)
Birth weight (g)	1,088 ± 340.3*
Caesarean section delivery	41 (63.0)
Postnatal factors	
Exposure to postnatal steroids	6 (9.2)*
Hypotension	37 (56.9)
Infant infection	26 (40.0)*
Patent ductus arteriosus	35 (53.8)
Necrotizing enterocolitis[c]	3 (4.6)
Duration ventilation (d)	3 (0–20)*
Chronic lung disease	13 (20.0)

[a]Data presented as number (%), or mean ± standard deviation.
[b]All subjects with maternal smoking (based on self-report) were exposed to marijuana, one was also exposed to tobacco.
[c]It was diagnosed based on Bell's stage II criteria [Kliegman et al., 1982].
*Statistical significance with respect to association with hindbrain growth ($P < 0.05$).

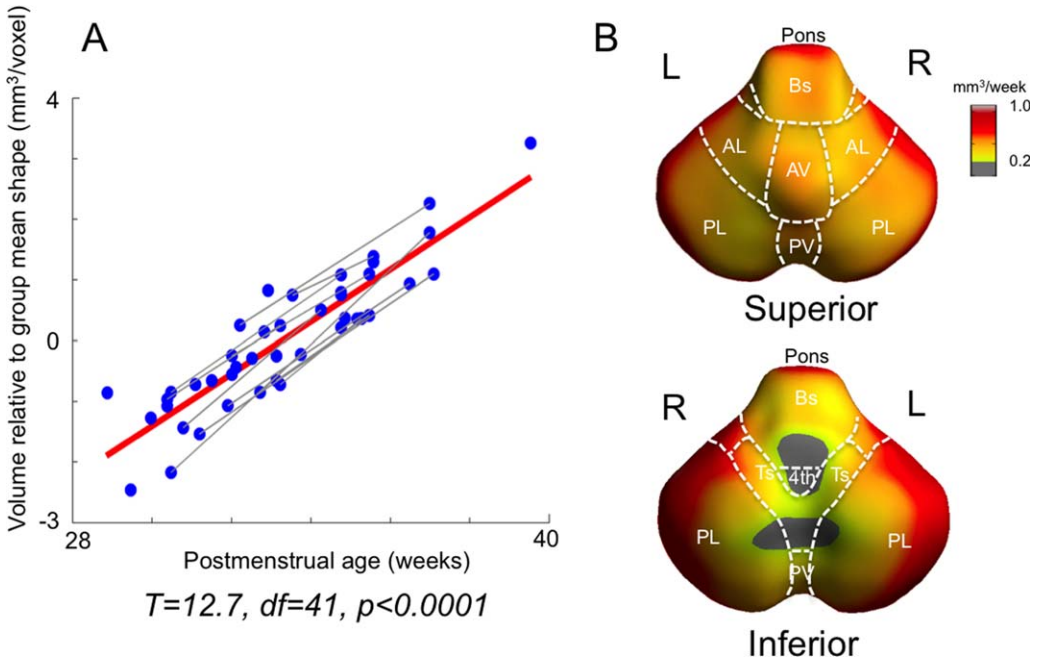

Figure 2.

Hindbrain growth in preterm neonates without brain injuries ($n = 30$). **A**. Significant mean growth estimated using a mixed-effect model. Gray lines represent serial scans of individuals, and red line represents overall group correlation. **B**. Normal growth rates (mm^3/wk). Voulme changes are shown within significant areas (corrected $P < 0.05$). AL/PL: anterior/posterior lobe; AV/PV: anterior/posterior vermis; Ts: Tonsil; Bs: brainstem (medulla); 4th: 4th ventricle; icp: inferior cerebellar peduncle. [Color figure can be viewed in the online issue, which is available at wileyonlinelibrary.com.]

impaired in association with moderate/severe intraventricular hemorrhage (IVH) and cerebellar hemorrhage (CbH).

Pattern of Hindbrain Growth in Preterm Born Neonates Without MR Evidence of Brain Injury

Based on phylogenetic and functional criteria, the cerebellum is primarily divided into three parts: vestibulocerebellum (consisting of flocculonodular lobe), spinocerebellum (consisting of vermis, paravermis, and fastigial/globose/emboliform nuclei), and cerebrocerebellum (consisting of cerebellar hemispheres and dentate nuclei). These regions are involved in different functions including regulation of motor tone, coordination, and cognition.

In the current study, cerebellar and brainstem growth in infants without MR evidence of brain injury varied across regions, which has been suggested by previous human postmortem and animal histological studies [Apps and Hawkes, 2009; Nowakowska-Kotas et al., 2014; Wang and Zoghbi, 2001]. The embryonic cerebellum develops from the dorsal region of the most rostral segment of the metencephalon (which will become the pons). Outgrowths in this area form the first elements of the cerebellum, which further develop towards the midline and merge in a rostral-to-caudal direction. These primitive hemispheres contact each other in the midline, forming the superior and inferior portions of the vermis. The lateral elements from this fusion finally develop into the cerebellar hemispheres [Wang and Zoghbi, 2001]. In our study, the pattern of postnatal cerebellar growth in which more rapid volume expansion is primarily mapped on the lateral surface, and corresponds well to the cerebellar morphogenesis that depicts development occurring earlier in the spinocerebellum and later in the lateral hemispheres. A recent study of human fetuses [Nowakowska-Kotas et al., 2014] has observed that the largest expansion of cerebellar surface at 26 to 30 weeks PMA occurs in the inferior region of anterior/posterior lobes. In this age range, the expansion of the posterior lobar surface was seen to be larger than in the anterior lobe. Our in vivo MRI data of preterm-born neonates confirm such characteristics of cerebellar growth that has been previously seen only in fetal postmortem data. We further observed a similar pattern of regional growth maintained postnatally up to 40 weeks PMA.

Relationship of Hindbrain Growth Impairment With Cerebral and Cerebellar Hemorrhage

We initially hypothesized that areas with fast growth postnatally may be more vulnerable to growth

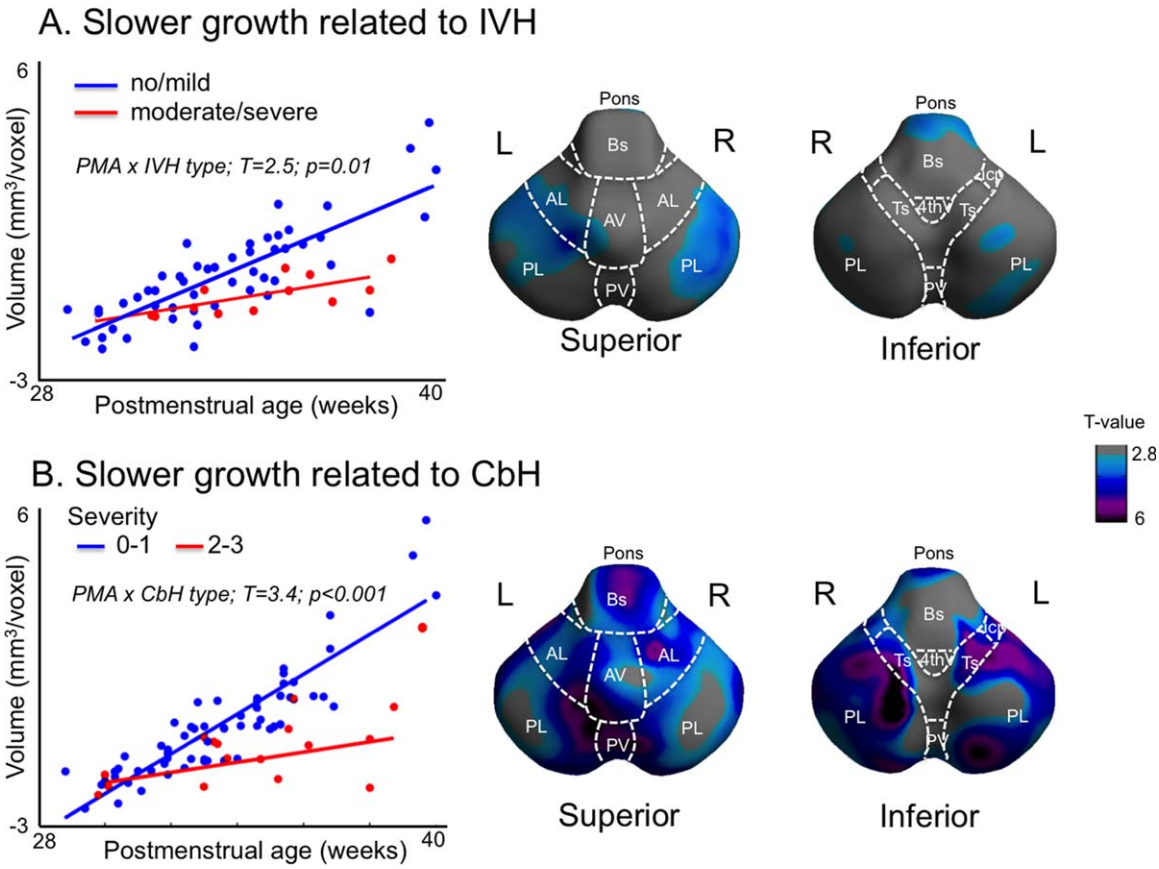

Figure 3.

Association between brain injuries and hindbrain growth. A mixed-effect model was used to account for multiple measurements per subject. Significantly slower growth related to severer intraventricular hemorrhage (IVH) was observed globally (**A**, left) and this change was mapped primarily to the posterior superior lobe and pons (A, right). Slower hindbrain growth was also associated with grade 2 and 3 of cerebellar hemorrhage (CbH) (**B**, left). Comparing the growth between neonates with grade 0 to 1 and those with grade 2 to 3, significantly slower growth in patients with severe CbH was observed extensively across regions (B, right). The largest changes were mapped to the posterior inferior lobe, posterior vermis, and tonsil. [Color figure can be viewed in the online issue, which is available at wileyonlinelibrary.com.]

impairment. Our observations confirmed that the regions displaying growth impairment were included in the regions displaying significant postnatal growth. However, they were not necessarily those with faster growth. We also found that the patterns of growth impairment varied depending on the type of related brain injuries (cerebral intraventicular hemorrhage versus cerebellar hemorrhage) as well as the sites of lesions (Figs. 3, 4). It is thus suggested that the mechanism involved in a given injury type may play a more important role in patterning of hindbrain dysplasia than postnatal growth rate.

In our study, the presence of CbH resulted in global cerebellar growth impairment, and the growth impairment was more pronounced in areas of hemorrhage. We showed that the pattern of CbH distributed mainly within shallow surface layers of the cerebellum in our patient cohort. Such a superficial zone likely represents hemorrhage from the external granular layer (EGL) which, as discussed earlier, is the germinal matrix for granule cells and other glutamatergic cells, which proliferate into the second postnatal year [Rakic and Sidman, 1970; Sidman and Rakic, 1973] and, therefore, requires a substantial blood supply [Sotelo, 2004; Wang and Zoghbi, 2001]. Neurogenesis in the EGL, particularly in the areas of posterior lobe and inferior cerebellar cortex that displayed a high frequency of CbH, is most active during the early third trimester [Sotelo, 2004; ten Donkelaar et al., 2003], at a postconceptional age equivalent to that of babies born prematurely. Although it is not clear whether these hemorrhages are primary (due to abnormal vessel walls) or secondary (with the primary injury, ischemic or otherwise, to the parenchyma), it must be assumed that local parenchymal hemorrhage reduces perfusion of the affected

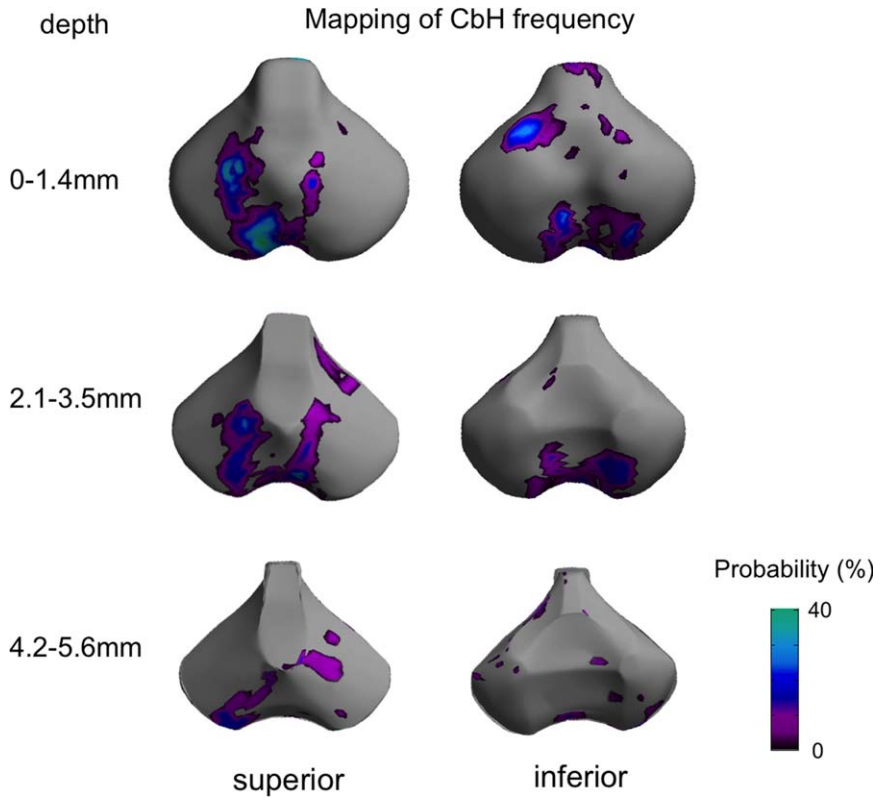

Figure 4.

Mapping of frequency of individual cerebellar hemorrhage (CbH). Volumes of the CbH graded 2 or higher are labeled and projected on to the surface sampled at every 0.7 mm (=size of a voxel) in depth from the original surface. For each individual the union was obtained between 0 and 1.4 mm, between 2.1 and 3.5 mm and between 4.2 and 5.6 mm. Shown are the frequencies of the projection of CbH in %. The CbH primarily distributes within superficial zones (0–3.5 mm) and the pattern largely overlaps with the pattern of growth impairment related to CbH shown in Figure 3B. [Color figure can be viewed in the online issue, which is available at wileyonlinelibrary.com.]

parenchyma. Therefore, neurogenesis in the EGL is likely to be disrupted in the presence of the hemorrhage, resulting in smaller regional volumes [Tam, 2013]. A study modeling postnatal CbH in mice [Yoo et al., 2014] showed a reduced rate in cerebellar growth during early postnatal development, associated with a decrease in granule cells, and persistent neurobehavioral abnormalities. Another possible mechanism for cerebellar growth impairment related to CbH is the neurotoxicity of blood products, including heme and free iron, which has been reported after intraparenchymal or subarachnoid hemorrhage in rodent models [Grojean et al., 2000; Nakamura et al., 2004; Yan et al., 2008].

Slower cerebellar growth was also associated with supratentorial hemorrhages and consequent IVH. However, the different pattern of impaired hindbrain growth in patients with cerebral IVH suggests a different mechanism than that related to CbH. It has been shown that cerebral IVH is associated with decreased cerebellar size at term and at age of 2 years in survivors of preterm birth. It is hypothesized that blood deposition in the fourth ventricle as a consequence of movement of blood after undergoing IVH has an effect on the cerebellar germinal zones that include the ventricular zone which produces GABAergic neurons, and the rhombic lips/external granular layer, which produce glutamatergic neurons [Tam et al., 2011b; Van Kooij et al., 2012]. The location of significant growth impairment related to IVH in our study included the superior lateral lobe and pons, which are relatively proximal to the fourth ventricle. Subarachnoid hemorrhage may also have an effect on the bone morphogenetic protein 2 and 4 (BMP2,4), which promotes cerebellar granule cell (glutamatergic neurons) formation in the rhombic lips and external granular layers [Haldipur et al., 2014]. Work of Haldipur et al. [2014] showed that impairment of function of FOXC1 in leptomeninges surrounding the developing cerebellum, SDF1alpha in developing cerebellum, or CXCR4 in ventricular zone (VZ) reduce VZ proliferation, leading to reduced production of Purkinje cells and the radial glial cells that direct Purkinje cell migration to the cerebellar cortex. Furthermore, low-grade IVH may result in cerebellar diaschisis

via Wallerian degeneration of white matter pathways to the cerebellar cortex and nuclei, leading to small cerebellar size [Morita et al., 2015].

Cerebellar growth could also be affected by cerebral injury, as loss of the numerous projections from the cerebral cortex to the cerebellar cortex (via the thalamus and pons) almost certainly has an effect on cerebellar development [Kiss et al., 2014]. The magnitude of this effect is currently unknown.

We found that the rate of hindbrain growth could be reduced with some clinical conditions, in particular exposure to postnatal steroid, duration of ventilation and birth weight. The association with the use of postnatal steroids in our latest 3 T MRI confirms the association found in our previous 1.5 T imaging study [Tam et al., 2011a]. Previous studies have also identified that cardiorespiratory factors such as consecutive intubation, hypotension, and patent ductus arteriosus are associated with hindbrain growth impairment [Argyropoulou et al., 2003; Messerschmidt et al., 2008]. Such compelling evidence suggests that the aforementioned clinical factors should be taken into account as potential covariates to clarify patterns of hindbrain growth impairment in prematurity and the related neurodevelopmental outcome although the pathophysiology remains to be investigated.

Technical Considerations, and Limitation of the Current Study and Future Direction

We recognize the following limitations to the current study. The analyzed local volume metric was relative to the constructed template, which limited a direct comparison with growth pattern reported in fetal ultrasound or postmortem studies. Many of the infants did not have MRI scans at the second time point due to back transport to their home facilities. For the second scan, most newborns were imaged a few days before their discharge. However, the discharge was sometimes made at the earliest day when the babies were deemed clinically stable, yielding a very few second scans near the term equivalent PMA. As a result the hindbrain growth reported here matches growth during the late third trimester. Another limitation is our inability to know which cells are affected in the cerebellar cortex (glutamatergic vs. GABAergic), whether the hemorrhages are cortical (as we presume) or subcortical, and precisely which parts of the brainstem and cerebrum are connected to the areas that are atrophic. We are currently investigating these questions by a wide angle of collaboration with neuropathologists who study the brains of premature infants in order to learn more about the histologic state of the premature cerebellar cortex and the location of the hemorrhages. Our on-going analysis of functional connectivity determined by resting-state fMRI may also yield information about the link between the location of hemorrhages and the type of the affected cells.

A very small proportion of babies had a conversion from "mild" injury on the initial MRI to "moderate" on the follow-up MRI (IVH = 0; WMI = 2; hydrocephalus = 1; CbH = 0). There was also one who had moderate WMI initially and was observed with mild WMI for the second scan. Because some supratentorial white matter injuries are quite small, and the identification, or lack thereof, of a single white matter lesion can result in a changed score, slight differences in the quality of the scan can result in change of the white matter score. However, because scans with significant motion artifact were excluded, this appeared to have no effect upon the study. In an additional analysis excluding those with converted severity, the WMI and hydrocephalus did not correlate with the pattern of hindbrain growth, and the effect of severity conversion upon our analysis was minimal. Finally, due to the very small sample size, we did not have the statistical power to assess the association between timing of injury and resultant hindbrain growth.

Investigation of the predictive values of the imaging measurements that proposed in the current study is of clinical importance. However, precise evaluation of neurodevelopmental outcome requires a long-term follow-up. Often, cognitive deficits in preterm-born survivors do not manifest until school age [Anderson et al., 2003; Bhutta et al., 2002]. We are currently evaluating neuromotor/cognitive performance in our cohort at serial time points and plan to continue long-term follow-up into adolescence.

CONCLUSION

This study is the first investigation of patterns of cerebellar growth in preterm newborns using in vivo MRI. The advanced morphometric analysis employed in the current study successfully identified different alterations of the normal cerebellar developmental trajectory that appear to result in different developmental outcomes in preterm infants with cerebellar (CbH) and cerebral (IVH) injuries, The patterns of altered cerebellar growth identified in our study confirm characteristics of cerebellar morphogenesis in perinatal development during the third trimester up to term-equivalent ages, previously observed only in histological data. Our proposed analytic framework has the potential to provide predictive imaging biomarkers for neurodevelopmental outcome, enabling early identification and treatment of high-risk patients.

REFERENCES

Almli CR, Rivkin MJ, McKinstry RC (2007): The NIH MRI study of normal brain development (Objective-2): Newborns, infants, toddlers, and preschoolers. Neuroimage 35:308–325.

Anderson P, Doyle LW, Victorian Infant Collaborative Study G (2003): Neurobehavioral outcomes of school-age children born extremely low birth weight or very preterm in the 1990s. JAMA 289:3264–3272.

Apps R, Hawkes R (2009): Cerebellar cortical organization: a one-map hypothesis. Nat Rev Neurosci 10:670–681.

Argyropoulou MI, Xydis V, Drougia A, Argyropoulou PI, Tzoufi M, Bassounas A, Andronikou S, Efremidis SC (2003): MRI measurements of the pons and cerebellum in children born preterm; associations with the severity of periventricular leukomalacia and perinatal risk factors. Neuroradiology 45:730–734.

Barkovich AJ, Kuzniecky RI, Jackson GD, Guerrini R, Dobyns WB (2001): Classification system for malformations of cortical development: Update 2001. Neurology 57:2168–2178.

Benjamini Y, Hochberg Y (1995): Controlling the false discovery rate: A practical and powerful approach to multiple testing. J Royal Stat Soc 57:289–300.

Bhutta AT, Cleves MA, Casey PH, Cradock MM, Anand KJS (2002): Cognitive and behavioral outcomes of school-aged children who were born preterm - A meta-analysis. JAMA 288: 728–737.

Blencowe H, Cousens S, Oestergaard MZ, Chou D, Moller AB, Narwal R, Adler A, Garcia CV, Rohde S, Say L, Lawn JE (2012): National, regional, and worldwide estimates of preterm birth rates in the year 2010 with time trends since 1990 for selected countries: A systematic analysis and implications. Lancet 379:2162–2172.

Chung MK, Worsley KJ, Nacewicz BM, Dalton KM, Davidson RJ (2010): General multivariate linear modeling of surface shapes using SurfStat. Neuroimage 53:491–505.

Dastjerdi FV, Consalez GG, Hawkes R (2012): Pattern formation during development of the embryonic cerebellum. Front Neuroanat 6:10.

Fonov V, Evans AC, Botteron K, Almli CR, McKinstry RC, Collins DL, Brain Development Cooperative G (2011): Unbiased average age-appropriate atlases for pediatric studies. Neuroimage 54:313–327.

Gerig G, Styner M, Jones D, Weinberg DR, Lieberman J (2001): Shape analysis of brain ventricles using SPHARM. MMBIA 171–178.

Geva R, Schreiber J, Segal-Caspi L, Markus-Shiffman M (2014): Neonatal brainstem dysfunction after preterm birth predicts behavioral inhibition. J Child Psychol Psychol 55:802–810.

Gilthorpe JD, Papantoniou EK, Chedotal A, Lumsden A, Wingate RJ (2002): The migration of cerebellar rhombic lip derivatives. Development 129:4719–4728.

Grojean S, Koziel V, Vert P, Daval JL (2000): Bilirubin induces apoptosis via activation of NMDA receptors in developing rat brain neurons. Exp Neurol 166:334–341.

Haldipur P, Gillies GS, Janson OK, Chizhikov VV, Mithal DS, Miller RJ, Millen KJ (2014): Foxc1 dependent mesenchymal signalling drives embryonic cerebellar growth. eLife 3:e03962.

Hoekstra RE, Ferrara TB, Couser RJ, Payne NR, Connett JE (2004): Survival and long-term neurodevelopmental outcome of extremely premature infants born at 23-26 weeks' gestational age at a tertiary center. Pediatrics 113:E1–E6.

Holland D, Chang LD, Ernst TM, Curran M, Buchthal SD, Alicata D, Skranes J, Johansen H, Hernandez A, Yamakawa R, Kuperman JM, Dale AM (2014): Structural growth trajectories and rates of change in the first 3 months of infant brain development. JAMA Neurol 71:1266–1274.

Imamura T, Ariga H, Kaneko M, Watanabe M, Shibukawa Y, Fukuda Y, Nagasawa K, Goto A, Fujiki T (2013): Neurodevelopmental outcomes of children with periventricular leukomalacia. Pediatr Neonatol 54:367–372.

Joo EY, Kim H, Suh S, Hong SB (2014): Hippocampal substructural vulnerability to sleep disturbance and cognitive impairment in patients with chronic primary insomnia: Magnetic resonance imaging morphometry. Sleep 37:1189–1198.

Kliegman RM, Hack M, Jones P, Fanaroff AA (1982): Epidemiologic-study of necrotizing enterocolitis among low-birth-weight infants - Absence of identifiable risk-factors. J Pediatr 100:440–444.

Kim H, Besson P, Colliot O, Bernasconi A, Bernasconi N (2008): Surface-based vector analysis using heat equation interpolation: A new approach to quantify local hippocampal volume changes. Med Image Comput Assist Interv 5241:1008–1015.

Kim H, Mansi T, Bernasconi N (2013): Disentangling hippocampal shape anomalies in epilepsy. Front Neurol 4:131.

Kiss JZ, Vasung L, Petrenko V (2014): Process of cortical network formation and impact of early brain damage. Curr Opin Neurol 27:133–141.

Knickmeyer RC, Gouttard S, Kang C, Evans D, Wilber K, Smith JK, Hamer RM, Lin W, Gerig G, Gilmore JH (2008): A structural MRI study of human brain development from birth to 2 years. J Neurosci 28:12176–12182.

Lind A, Parkkola R, Lehtonen L, Munck P, Maunu J, Lapinleimu H, Haataja L, Group PS (2011): Associations between regional brain volumes at term-equivalent age and development at 2 years of age in preterm children. Pediatr Radiol 41:953–961.

Messerschmidt A, Prayer D, Brugger PC, Boltshauser E, Zoder G, Sterniste W, Pollak A, Weber M, Birnbacher R (2008): Preterm birth and disruptive cerebellar development: Assessment of perinatal risk factors. Eur J Paediatr Neurol 12:455–460.

Miller SP, Cozzio CC, Goldstein RB, Ferriero DM, Partridge JC, Vigneron DB, Barkovich AJ (2003): Comparing the diagnosis of white matter injury in premature newborns with serial MR imaging and transfontanel ultrasonography findings. AJNR Am J Neuroradiol 24:1661–1669.

Miller SP, Ferriero DM, Leonard C, Piecuch R, Glidden DV, Partridge JC, Perez M, Mukherjee P, Vigneron DB, Barkovich AJ (2005): Early brain injury in premature newborns detected with magnetic resonance imaging is associated with adverse early neurodevelopmental outcome. J Pediatr 147:609–616.

Morita T, Morimoto M, Yamada K, Hasegawa T, Morioka S, Kidowaki S, Moroto M, Yamashita S, Maeda H, Chiyonobu T, Tokuda S, Hosoi H (2015): Low-grade intraventricular hemorrhage disrupts cerebellar white matter in preterm infants: Evidence from diffusion tensor imaging. Neuroradiology 57: 507–514.

Nakamura T, Keep RF, Hua Y, Schallert T, Hoff JT, Xi G (2004): Deferoxamine-induced attenuation of brain edema and neurological deficits in a rat model of intracerebral hemorrhage. J Neurosurg 100:672–678.

Nowakowska-Kotas M, Kedzia A, Dudek K (2014): Development of external surfaces of human cerebellar lobes in the fetal period. Cerebellum 13:541–548.

Papile LA, Burstein J, Burstein R, Koffler H (1978): Incidence and evolution of subependymal and intraventricular hemorrhage: A study of infants with birth weights less than 1,500 gm. J Pediatr 92:529–534.

Parker J, Mitchell A, Kalpakidou A, Walshe M, Jung HY, Nosarti C, Santosh P, Rifkin L, Wyatt J, Murray RM, Allin M (2008): Cerebellar growth and behavioural & neuropsychological outcome in preterm adolescents. Brain 131:1344–1351.

Payne AH, Hintz SR, Hibbs AM, Walsh MC, Vohr BR, Bann CM, Wilson-Costello DECEKSNI (2013): Neurodevelopmental outcomes of extremely low-gestational-age neonates with low-

grade periventricular-intraventricular hemorrhage. JAMA Pediatr 167:451–459.

Rakic P, Sidman RL (1970): Histogenesis of cortical layers in human cerebellum, particularly the lamina dissecans. J Comp Neurol 139:473–500.

Sato K, Ishigame K, Ying SH, Oishi K, Miller MI, Mori S (2015): Macro- and microstructural changes in patients with spinocerebellar ataxia type 6: assessment of phylogenetic subdivisions of the cerebellum and the brain stem. Am J Neuroradiol, 36:84–90.

Sidman RL, Rakic P (1973): Neuronal migration, with special reference to developing human brain: a review. Brain Res 62:1–35.

Skiold B, Alexandrou G, Padilla N, Blennow M, Vollmer B, Aden U (2014): Sex differences in outcome and associations with neonatal brain morphology in extremely preterm children. J Pediatr 164:1012–1018.

Sled JG, Zijdenbos AP, Evans AC (1998): A nonparametric method for automatic correction of intensity nonuniformity in MRI data. IEEE Trans Med Imaging 17:87–97.

Sotelo C (2004): Cellular and genetic regulation of the development of the cerebellar system. Prog Neurobiol 72:295–339.

Styner M, Oguz I, Xu S, Brechbühler C, Pantazis D, Gerig G (2006): Statistical Shape Analysis of Brain Structures Using SPHARM-PDM. MICCAI 2006 Opensource workshop.

Tam EW, Chau V, Ferriero DM, Barkovich AJ, Poskitt KJ, Studholme C, Fok ED, Grunau RE, Glidden DV, Miller SP (2011a): Preterm cerebellar growth impairment after postnatal exposure to glucocorticoids. Sci Transl Med 3:105ra105.

Tam EW, Miller SP, Studholme C, Chau V, Glidden D, Poskitt KJ, Ferriero DM, Barkovich AJ (2011b): Differential effects of intraventricular hemorrhage and white matter injury on preterm cerebellar growth. J Pediatr 158: 366–371.

Tam EWY (2013): Potential mechanisms of cerebellar hypoplasia in prematurity. Neuroradiology 55:41–46.

ten Donkelaar HJ, Lammens M, Wesseling P, Thijssen HO, Renier WO (2003): Development and developmental disorders of the human cerebellum. J Neurol 250:1025–1036.

Van Braeckel KNJA, Taylor HG (2013): Visuospatial and visuomotor deficits in preterm children: The involvement of cerebellar dysfunctioning. Dev Med Child Neurol 55:19–22.

Van Kooij BJM, Benders MJNL, Anbeek P, Van Haastert IC, De Vries LS, Groenendaal F (2012): Cerebellar volume and proton magnetic resonance spectroscopy at term, and neurodevelopment at 2 years of age in preterm infants. Dev Med Child Neurol 54:260–266.

Wang VY, Zoghbi HY (2001): Genetic regulation of cerebellar development. Nat Rev Neurosci 2:484–491.

Yan J, Chen C, Hu Q, Yang X, Lei J, Yang L, Wang K, Qin L, Huang H, Zhou C (2008): The role of p53 in brain edema after 24 h of experimental subarachnoid hemorrhage in a rat model. Exp Neurol 214:37–46.

Yoo JYJ, Mak GK, Goldowitz D (2014): The effect of hemorrhage on the development of the postnatal mouse cerebellum. Exp Neurol 252:85–94.